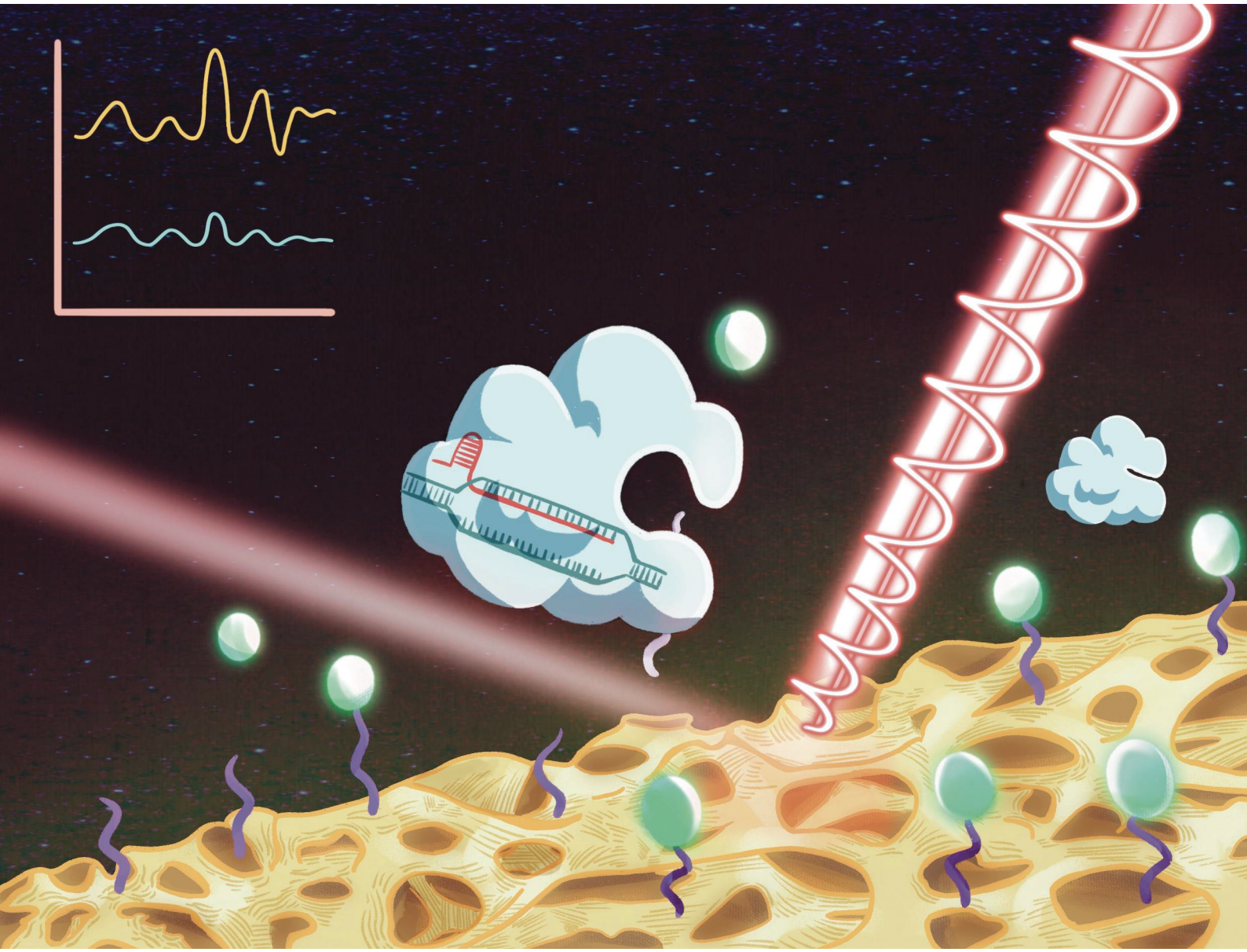
Volume 149
Number 17
7 September 2024
Pages 4313-4526

Analyst

rsc.li/analyst



ISSN 0003-2654

PAPER

Yu Zhao *et al.*

A CRISPR/Cas12a-powered gold/nickel foam surface-enhanced Raman spectroscopy biosensor for nucleic acid specific detection in foods

Image credit: JM Shen (SHNU), ZX Zhao (NYHS), LD Kong (SHNU) and QQ Li (BN Med)

ROYAL SOCIETY OF CHEMISTRY

Analyst

PAPER

Check for updates

Cite this: *Analyst*, 2024, **149**, 4343

A CRISPR/Cas12a-powered gold/nickel foam surface-enhanced Raman spectroscopy biosensor for nucleic acid specific detection in foods†

Yan Liu,[a] Shirui Gou,[b] Long Qiu,[c] Zhiwen Xu,[d] Haifeng Yang,[a] Shiping Yang[a] and Yu Zhao*[b]

Received 31st May 2024,
Accepted 14th July 2024

DOI: 10.1039/d4an00778f

rsc.li/analyst

Food is a necessary source of energy, but it also serves as a pathway for transmitting infectious pathogens, making food safety a matter of great concern. Rapid, accurate, and specific detection methods for food-borne viruses are crucial. Surface-Enhanced Raman Scattering (SERS), due to its superior sensitivity and characteristic fingerprint spectra, holds enormous potential. However, due to the limitations of SERS, it requires specific conditions to achieve specificity. In order to enhance the specificity and accuracy of nucleic acid detection based on SERS, we have developed a CRISPR-Cas12a-mediated SERS technique to identify target DNA, harnessing the targeting recognition capability of CRISPR-Cas12a and ultra-sensitive SERS tags and successfully addressing SERS' lack of specific detection capability. This system includes a gold/nickel foam substrate (Au-NFs) and a reporter (ssDNA–ROX). The phenomenon of colloidal gold/silver nano-aggregation due to magnesium ions, which is commonly encountered in CRISPR-SERS, was simultaneously solved using AuNFs. The qualitative and quantitative analysis of target DNA in drinking water was performed by monitoring the intensity change of ROX Raman reporter molecules. The results showed that the sensor detected DNA within 30 min and the limit of detection (LOD) was 8.23 fM. This is expected to become one of the alternative methods for nucleic acid detection for its rapid detection and high specificity.

1. Introduction

Food, as a vehicle for the transmission of foodborne viruses,[1] directly impacts public health. Therefore, ensuring food safety is a critically important task. Foodborne diseases caused by the ingestion of food contaminated by pathogenic microorganisms and toxic chemicals pose a significant threat to human health.[2] Foodborne viruses are one of the leading causes of foodborne diseases.[3] Foodborne diseases account for 7.5% of annual deaths (56 million deaths).[4,5] These viruses can be transmitted from infected humans or animals to a new host by several routes.[6] Thus, their detection and identification are crucial for the prevention of outbreaks of foodborne diseases.[7,8] Traditional methods for detecting foodborne pathogens rely on microbial isolation, culture, and biochemical identification techniques.[9,10] However, these traditional methods for microbial detection and the identification of foodborne pathogens are both time-consuming and laborious.[11,12] It is very urgent to improve the detection level of food-borne pathogens and ensure food safety.[13,14] Among them, Hepatitis A Virus (HAV) is one of the biggest causes of outbreaks of foodborne diseases in the world. The Hepatitis A Virus (HAV) has a major impact on public health and is considered the most important human foodborne pathogen in the Western world. The main routes of HAV transmission usually occur *via* the fecal–oral route, the ingestion of contaminated food and water, and direct human-to-human contact.[15] Therefore, there is an increasing need to design a new strategy for rapid, accurate, sensitive, and economical detection of foodborne HAV in foods.

Raman scattering is an inelastic process that takes advantage of the unique vibrations generated by individual bonds to produce a specific spectrum of molecules. Each molecule has its own characteristic Raman spectrum.[16] SERS (Surface-Enhanced Raman Spectroscopy) is when a molecule is adsorbed to a rough metal surface (such as silver or gold nanoparticles (NPs)), the inelastic light scattering of the molecule is greatly enhanced, and in some cases, single-molecule level detection can be achieved.[17] The enhancement mechanism of

[a]*College of Chemistry and Materials Science, Shanghai Normal University, Shanghai, China*
[b]*College of Life Sciences, Shanghai Normal University, Shanghai, China*
[c]*Wuxi Tolo Biotechnology Co., Ltd, Wuxi, Jiangsu, China*
[d]*Technology Center for Animal Plant and Food Inspection and Quarantine of Shanghai Customs, Shanghai, China*

† Electronic supplementary information (ESI) available. See DOI: https://doi.org/10.1039/d4an00778f

SERS is generally divided into two categories: one is surface plasmon resonance, which increases the electric field intensity of the incident light, and this mechanism is called electromagnetic field enhancement, also called physical enhancement; the other is called chemical enhancement, which increases the polarizability of molecules.[18] SERS has been widely used for the detection of biomolecules, including proteins,[19] DNA,[20,21] and cells.[22] SERS detection is highly sensitive, non-destructive, is capable of small sample detection and rapid detection, and is suitable for the detection of samples in a variety of states and types (solids, liquids, and gases).[23,24] More importantly, if equipped with portable Raman devices, rapid field detection can be performed.[25] Rapid detection is also useful in the diagnostic assessment and personalized treatment of infectious diseases.[26,27] In the detection of food-borne viruses, SERS technology can achieve the rapid detection of extremely trace-level virus particles, which is expected to play an important role in early diagnosis and epidemic surveillance. However, the surface of foodborne viruses contains phospholipids and proteins, and the complex binding of these molecules is different between each cell.[28] Direct contact of biomacromolecules with the bare metal usually results in denaturation and poor reproducibility of SERS.[18] Therefore, direct and label-free detection of unmodified DNA has been a great challenge for DNA analysis.[29] The SERS technique is seldom used for qualitative and quantitative detection in food samples due to its lack of selectivity for the chemical composition of the sample. This reduces its reliability and accuracy in practical applications.[24] Therefore, improving the specificity and sensitivity of SERS biosensors is necessary to enhance their application in virus detection.

CRISPR (Clustered Regularly Interspaced Short Palindromic Repeats) is a revolutionary gene editing technology. CRISPR technology is derived from the natural immune system of bacteria, which is utilized by bacteria to fight off viral infections.[30–32] In recent years, CRISPR technology has become one of the hottest research fields in the life sciences and has been reported in the fields of medicine, environment, agriculture, *etc*.[33–37] CRISPR technology strictly follows the principle of base-pairing and provides a powerful detection tool for the targeted detection of nucleic acids, with a high degree of specificity.[38–40] Cas12a, a variant of the CRISPR-Cas gene editing system, has a unique "nuclease activity" that recognizes and cleaves the target DNA and then cuts non-specific single-stranded DNA (ssDNA) molecules.[41] Utilizing this *trans*-cleavage property, when activated, Cas12a cleaves these probes, releasing a fluorescent signal that enables signal amplification.[42–44] Therefore, utilizing the recognition mechanism of CRISPR can reduce the probability of false positives and false negatives, and combining it with SERS technology is expected to improve the low specificity and non-selectivity of SERS technology in nucleic acid detection. Therefore, the combination of CRISPR and SERS technology is expected to improve the specificity and sensitivity of biosensors and to be faster than traditional PCR methods.[45] Several studies have demonstrated the superiority of CRISPR in combination with SERS for nucleic acid detection. For example, Jin-Ha Choi *et al.* modified ssDNA outside of AuNPs to form RAuNPs probes and immobilized them on activated graphene oxide (GO)/periodic triangular gold nanoflower (TANF) arrays. It achieves Jin-Ha Choi *et al.* modified ssDNA outside of AuNPs to form RAuNPs probes and immobilized them on activated graphene oxide (GO)/periodic triangular gold nanoflower (TANF) arrays. It achieves sensitive and specific detection of hepatitis B virus (HBV), human papillomavirus 16 (HPV-16) and HPV-18 multiviral DNAs.[46] Pang *et al.* established a lateral flow technique based on CRISPR-Cas12a specific recognition capability and ultra-sensitive SERS labeling for the detection of double-stranded DNA and single-base localization. The outcomes demonstrated that compared to the conventional colorimetric LFA approach, the detection efficiency was higher.[47] The CRISPR–SERS biosensor shows the potential to achieve specificity, sensitivity and rapid detection of DNA.

In this paper, high specificity of the detection was achieved using CRISPR. A CRISPR-SERS sensor is proposed based on study of the CRISPR-SERS sensing mechanism. We employed CRISPR-Cas12a to specifically recognize the target HAV-cDNA and integrated ssDNA–ROX on the AuNF surface. The presence or absence of target DNA was determined by detecting changes in the SERS intensity of the signaling molecule ROX on the AuNF surface. Utilizing the high specificity of CRISPR and the high sensitivity of the SERS detection method, a CRISPR-SERS biosensor was developed for the rapid and selective detection of nucleic acids. Using nickel foam as a template, gold nanocones with a large number of spikes were grown on the nickel foam by the chemical substitution reaction between chloroauric acid and nickel metal, and their SERS properties were evaluated. ROX–ssDNA was immobilized on AuNFs due to the sulfhydryl group that can form an Au–S bond with gold as a SERS label. The target DNA was used to activate the *trans*-conjugation cleavage activity of Cas12a to shear ssDNA on AuNFs. Qualitative and quantitative analysis of HAV-cDNA was carried out by monitoring the Raman intensity changes of ROX signaling molecules. AuNFs is a flexible material with a honeycomb and three-dimensional mesh structure, with small pore size and density, with a certain roughness and large specific surface area. Nickel foam was used as a template, and the chemical displacement reaction between chloro-auric acid and nickel metal was used to grow gold nanocones on the nickel foam. The directly grown gold/silver nanostructures on the nickel foam could contain more "hot spot" molecules in the three-dimensional focusing volume, thus increasing the intensity of the SERS signal.[48–51] Because the electromagnetic field around the nanostructure is not evenly distributed, but highly localized in the spatial narrow area, such as at the tip, the gap will produce greater electromagnetic field enhancement.[52] At the same time, there is a "lightning rod effect" at the tip, so the growth of gold on the nickel foam to form a nanocone shape can produce a greater electromagnetic field enhancement and improve the SERS effect.[53] In addition, divalent magnesium ions play a very important role in the construction of Cas12a/gRNA/target DNA ternary complexes, which is necess-

 This journal is © The Royal Society of Chemistry 2024

ary for effective crRNA binding.[54] The optimal concentration of magnesium ions ranged between 10 mM and 12 mM.[55] The presence of this magnesium ion concentration is lethal to conventional nanoparticle colloids, causing excessive aggregation of colloidal gold/silver, thus affecting the base SERS enhancement. It is very difficult to affect neither the CRIPSR reaction nor the SERS detection, and the growth of gold nanocones on the surface of the 3D flexible nickel foam used in this study can effectively solve this problem. The effect of precious metal nanoparticle aggregation caused by the presence of inorganic ions in the CRISPR system was avoided.

2. Materials and methods

2.1. Materials and apparatus

Chloroauric acid ($HAuCl_4$, Pure Analytical), concentrated ammonia water and PBS (pH = 7.4) were purchased from Sangon Biotech (Shanghai) Co., Ltd. Foam nickel (aperture 0.23 mm, thickness 0.3 mm, Suzhou Christie Foam Metal Co., Ltd) was washed with water and set aside. The glassware was soaked in aqua regia solution (hydrochloric acid : nitric acid = 3 : 1) for 24 hours, washed with water several times, and dried for future use.

Reporter-FQ and SERS reporter (ssDNA–ROX) were synthesized and HPLC purified by Sangon Biotech (Shanghai) Co., Ltd. HAV-cDNA, HBV, NOV GI, NOV GII, crRNA, LbCas12a (ToloBio, China), NEBuffer 2.1 and UltraPure™ DNase/RNase-Free Distilled Water (ThermoFisher, USA) were obtained from Shanghai Tolo Biotech Co., Ltd.

The morphology and element composition distribution of the Au-NFs composite substrate were characterized by scanning electron microscopy (ZEISS GeminiSEM 300, Germany). Raman measurements were performed using the Portable Raman system (Zolix, China) equipped with a 785 nm laser. The excitation source of the Raman spectrometer consists of a diode laser with a wavelength of 785 nm and a maximum adjustable power of 300 mW. The exposure time of each spectral acquisition was 2 s, and the cumulative number was 3. The amplification step was performed through a fluorescent quantitative PCR detection system (Biogener Q3202, Hangzhou Biogener Technology Co., Ltd, Hangzhou, China). The DNA used in this study was quantified using a DeNovx DS-11 spectrophotometer.

2.2. Preparation of a magnetic composite SERS substrate

First, the nickel foam was cut into small pieces (0.25 × 0.25 cm^2) with scissors. At room temperature, the nickel foam sheet was soaked in concentrated ammonia water for 30 min to remove the surface oxide layer to show a metallic luster. After washing, the nickel foam sheet was allowed to stand in 1% $HAuCl_4$ solution and reacted for 10 min before magnetic separation, and Au-NFs slices were obtained with water. The synthesized thiol reporter probe was dissolved in TE buffer (Tris–HCl (10 mM), EDTA (1 mM), pH = 8.0) and incubated at 37 °C for 30 min. The SERS substrate was kept at 4 °C for the final use.

2.3. Optimization of the SERS biosensor

The self-assembly reaction time of chloroauric acid and nickel foam was optimized.

The ssDNA–ROX was incubated with foam nickel–gold for 30 min at room temperature. The standard solution of the signal molecule ssDNA–ROX was diluted to obtain analytical solutions of different concentrations. Au-NFs were immersed in it, which was magnetically separated after standing for 1 h, and excess liquid was absorbed with absorbent paper for SERS detection. The reaction times and different concentrations of signal molecules were optimized.

2.4. CRISPR system

LbCas12a, crRNA, NEBuffer 2.1, and the ROX–ssDNA signal reporter probe make up the CRISPR system. The Cas12a protein's *trans*-cleavage activity is triggered in the presence of the target DNA. The CRISPR/Cas12a complex in this instance is made up of 1 μL of target DNA, 500 nM Cas12a, 250 nM crRNA, and 5 μL of NEBuffer 2.1. The cut time was optimized. To validate this assay strategy, fluorescence validation was introduced by adding 200 nM ssDNA–FQ and then incubating at 37 °C for 16 min, with fluorescence measurements taken every 2 min. The fluorescence signal in the presence of different components was also tested.

2.5. Detection of the HAV-cDNA by the Raman system

The ssDNA–ROX signaling probe was loaded on the AuNFs SERS substrate and washed with UltraPure™ DNase/RNase-Free Distilled Water (ThermoFisher, USA) before use. After that, the substrate and 20 μL of the CRISPR/Cas12a complex were incubated for 30 minutes at 37 °C to allow the process to finish. The substrate was gently cleaned three times with UltraPure™ DNase/RNase-Free Distilled Water before the Raman measurement. The Raman test parameters are: the laser light source wavelength is 785 nm; the laser power is 180 mV; and the wavelength range of the collected data is 500–2000 cm^{-1}.

2.6. Application of CRISPR-SERS biosensors in real samples

The bottled water used in this study was purchased from the local market. According to the SN/T 4784-2017 Industry Standard for Entry–Exit Inspection and Quarantine of the People's Republic of China, the pretreatment method of bottled water is to filter 500 mL with a Millipore Filter Membrane with a diameter of 50 mm and a pore diameter of 0.45 μm. The solution pH was adjusted to 7.0 with a 0.1 mol L^{-1} hydrochloric acid solution. The samples were prepared for artificial contamination with different concentrations of HAV-cDNA.

2.7. Data analysis

Raman map data in the text were baseline corrected, smoothed and normalized with LabSpec5.0 and then graphed with origin

2016. Baseline correction can eliminate interference from the fluorescence background and instrument noise. The stoichiometric statistical analysis method of principal component analysis (PCA) combined with the linear discriminant analysis (LDA) method was used to establish the identification model of SERS spectra and category information of foodborne pathogenic bacteria. All the statistical analyses in the experiment were carried out using Origin software.

3. Results and discussion

3.1. CRISPR-SERS biosensor strategy

Fig. 1 shows the strategy for detecting HAV-cDNA using the CRISPR-SERS biosensor. First, Cas12a–crRNA recognizes the target HAV-cDNA using a T-rich PAM (protospacer adjoining motif) sequence complementary to the target sequence.

The target sequence of the HAV-cDNA is recognized by the complementarity of the Cas12a–crRNA to the target sequence. When the target DNA is present, Cas12a not only cuts the target DNA in *cis*, but also cuts the non-target ssDNA in *trans*, and randomly shears the surrounding ssDNA; in this case, Cas12a acts like "scissors" to cut the ssDNA (ssDNA–ROX signal probe) linked to the AuNFs. After washing, the signal molecule ROX is released from the system, and the characteristic ROX lambda intensity decreases (1503 cm^{-1}). On the other hand, because of the absence of target DNA, Cas12a–crRNA cannot be activated, cannot decode the target DNA, and cannot cut the surrounding ssDNA-linked signal molecule, so it can only remain in its original position. At this point, the Raman peak intensity of the signal molecule ROX remains almost unchanged. The strategy used in the whole characterization process is "signal off". The combination of CRISPR recognition and SERS detection provides a super-specific and sensitive sensing mechanism, making DNA recognition and detection efficient and specific, providing a powerful and robust tool for the detection of HAV-cDNA. To improve the detection sensitivity of the CRISPR-SERS biosensor, gold nanocones grown on the nickel foam surface generate more Raman "hot spots", thus increasing the sensitivity of the sensor. By providing a strong localized electric field, the Raman signals of nearby target molecules are enhanced; this fundamentally explains the combination of the CRISPR-SERS sensor with an ultrasensitive sensing mechanism.

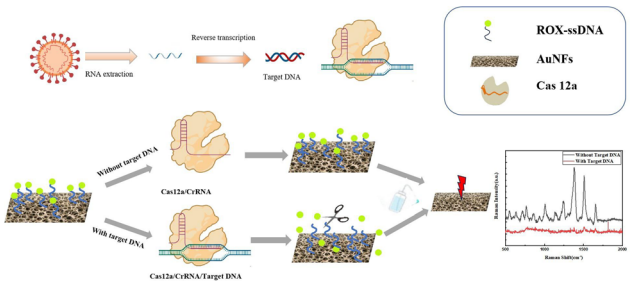


Fig. 1 Schematic diagram of the nucleic acid detection strategy of the CRISPR-SERS biosensor. After the binding of the target DNA to the Cas12a–crRNA duplex, it is directly used to trigger the CRISPR system. When the target DNA is present, the *trans*-cleavage activity of Cas12a to the non-specific ssDNA reporter is activated, and the Raman signal reporter consisting of ssDNA and ROX molecules will be cut into small fragments. A decrease in Raman intensity was observed after the ROX molecules were eluted from the SERS substrate. In contrast, in the absence of target DNA, Cas12a/crRNA does not initiate the *trans*-cleavage activity of the ssDNA–ROX reporter probe, resulting in virtually undetectable changes in the Raman signal.

3.2. SERS substrate characterization

The substrate of surface-enhanced Raman spectroscopy is crucial to initiating the SERS effect. AuNFs were characterized using scanning electron microscopy (SEM). As shown in Fig. 2A, a honeycomb, three-dimensional mesh structure can be seen. As can be seen in Fig. 2B and C, the gold nanocones growing on the surface of nickel foam are evenly distributed on the surface. As can be seen in Fig. 2D, the substrate has a regular gold nanocone structure, and the size of the nanocone is about 500 nm. According to the SERS electromagnetic field enhancement mechanism, metal nanoparticles with large specific surface areas will produce "hot spots" at the particle tip, which facilitates the formation of local plasmonic field hot spots. There are smaller gaps between the particles, which can not only generate "hot spots" again but also adsorb a large number of signal molecules to further amplify the signal.

3.3. Feasibility analysis of the CRISPR-SERS biosensor detecting HAV-cDNA

As illustrated in Fig. 3A, the presence of target DNA triggers indifferent cleavage characteristics of Cas12a, resulting in the formation of a ternary complex that includes Cas12a, crRNA, and target DNA. Reduced Raman intensity is observed at the distinctive ROX peaks when ROX molecules that are in close proximity to the substrate are washed away. Fluorescence verification was performed using a 5 '6-FAM, 3' BHQ1 labeled

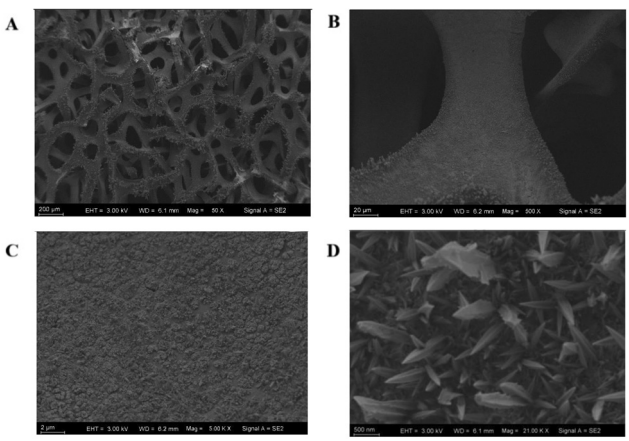


Fig. 2 The SEM image of the same material magnified step by step. (A) Magnetic composite SEM of AuNFs under low magnification; (B and C) AuNFs under high magnification – the surface becomes rough; and (D) needle nano-gold under high magnification.

This journal is © The Royal Society of Chemistry 2024

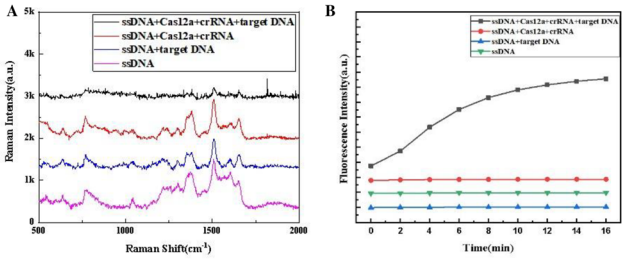


Fig. 3 (A) Feasibility analysis of the CRISPR-SERS biosensor in HAV-cDNA detection shows that it reduces the Raman intensity if and only when Cas12a, crRNA, and target DNA are present and (B) fluorescence validation of the CRISPR-based biosensor in HAV-cDNA detection.

signal reporting probe (FQ-ssDNA, 200 nM). Target DNA was evaluated in order to determine the function of Cas12a, crRNA, and the three fundamental parts of the CRISPR system. Fig. 3B demonstrates that the fluorescence intensity of FQ–ssDNA only increases with reaction time when all three components are present in the solution. In conclusion, these findings show that the CRISPR platform can be used to detect HAV-cDNA.

3.4. CRISPR-SERS biosensor preparation and the optimization of detection conditions

The key factor for the *in situ* synthesis of nickel-foam/gold is the reduction time. The nickel-foam/gold reaction time was optimized, as shown in Fig. 4A, with the strongest SERS signal at 10min. The amount of ssDNA–ROX probe that sticks to the substrate greatly affects the CRISPR-SERS biosensor probes' sensitivity and stability.[56] The optimal signaling probe concentration is determined by the intensity of the Raman peak at 1503 cm^{-1}. The fixed signaling probe concentration varied from 10 nM to 100 nM, 500 nM, 1000 nM, and 2000 nM. Fig. 4B shows how the associated Raman intensity gradually increased until it reached a high point. For economic reasons, 1000 nM ssDNA–ROX was used in the following studies. AuNFs react with the Au–S bond and signal probe ssDNA–ROX, and the reaction time is too short and insufficient to reach the maximum efficiency; too long a reaction time will increase the number of uncontrollable results. As a result, Fig. 4C illustrates how the nickel foam/gold reaction time was tuned with the signal probe molecule, with 40 minutes being the ideal reaction time. Another important feature that significantly influences the CRISPR-SERS biosensor's reliability is the moment at which the as12a protein cuts the ssDNA–ROX probe.[57] The ideal reaction time for cleavage was determined to be 30 minutes, as demonstrated in Fig. 4D, where a rise in ΔI% (intensity change) occurred as the reaction time increased from 10 to 30 minutes, stabilizing at 25 minutes and extending to 35 minutes.

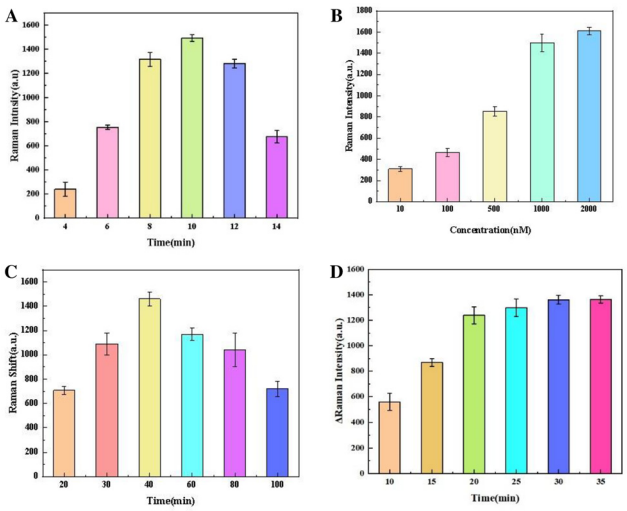


Fig. 4 (A) Optimization of the reaction time of chlorogenic acid and nickel foam; (B) optimization of signal molecule concentration; (C) optimization of the reaction time of signal molecule ssDNA–ROX with nickel–gold foam. (D) Cleavage time optimization (error bar data for 5 points per sample).

3.5. Performance analysis of the CRISPR-SERS biosensors

Under optimized conditions, the created CRISPR-SERS biosensor was able to detect different amounts of HAV-cDNA. The results in Fig. 5A show that the Raman intensity gradually decreases with increasing concentration of HAV-cDNA. In Fig. 5B, the range 2.39×10^{-9} to 4.78×10^{-13} mol L^{-1} shows that the logarithm of ΔI (intensity change) and HAV-cDNA concentration are observed; the regression equation is $Y = 287.10X + 3801.68$ ($R^2 = 0.9908$), where Y and X represent the logarithm of change in Raman signal value ΔI and HAV-cDNA concen-

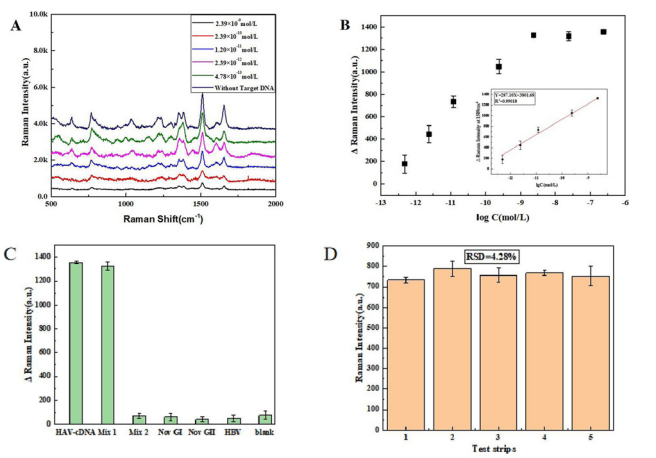


Fig. 5 (A) Raman spectra of 2.39×10^{-9}, 2.39×10^{-10}, 1.20×10^{-11}, 2.39×10^{-12} and 4.78×10^{-13} M. (B) The ΔRaman intensity of the log of the different HAV-cDNA concentrations. Small plots show the linear relationship of the log of HAV-cDNA concentration. Error bars represent means ± SD, where for replicates $n = 5$. (C) Selectivity of the developed CRISPR-SERS for the HAV-cDNA. All the negative and blank groups caused only relatively small intensity changes. Mix 1: HAV-cDNA, Nov GI-cDNA, Nov GII-cDNA, and HBV; mix 2: Nov GI-cDNA, Nov GII-cDNA, and HBV. (D) The SERS repeatability of 120 pM target HAV-cDNA was detected. Error bars represent the standard deviation ($n = 3$).

Table 1 Results of the recovery test for HAV-cDNA in bottled water

Test/group number	Spiked HAV-cDNA concentration (mol L^{-1})	The HAV-cDNA concentration measured by this method (mol L^{-1})	Recovery rate (%)	Average recovery rate (%)	The HAV-cDNA concentration measured by RT-qPCR (mol L^{-1})
1	2.390×10^{-10}	2.440×10^{-10}	102.09	107.99	
		2.614×10^{-10}	109.37		2.367×10^{-10}
		2.689×10^{-10}	112.51		
2	1.200×10^{-12}	1.263×10^{-12}	105.25	102.44	
		1.198×10^{-12}	99.83		1.139×10^{-12}
		1.227×10^{-12}	102.25		
3	1.200×10^{-14}	0.9708×10^{-14}	80.90	82.23	
		0.9855×10^{-14}	82.13		1.230×10^{-14}
		1.004×10^{-14}	83.67		

tration, and the detection limit is 8.23 fM (calculated by the ratio of the 3 fold standard deviation value of the blank and the slope of the standard curve). This value is the same order of magnitude (as shown in Table S2†) as the recently reported CRISPR/Cas12a-based SERS detection method. And the time is even shorter. Compared with other SERS-based nucleic acid detection methods, this method is more sensitive, has more convenient detection, and avoids a complex and demanding amplification step.

Simulating the complexity of the real test setting, two mixed viruses (containing and lacking HAV-cDNA) were tested simultaneously along with positive and negative control groups. The results are displayed in Fig. 5C, where the excellent specificity of the assay is confirmed by the large increases in intensity values given by all positive groups, even the material mixed with HAV-cDNA (mix 1). The ΔRaman intensity of the positive group was roughly 13 times higher than that of the negative group.

3.6. Recovery test

To explore the potential application of this biosensor in real food samples, we evaluated the method by real sample spike recovery experiments. The experiments were performed according to the SN/T 4784-2017 Entry–Exit Inspection and Quarantine Industry Standard of the People's Republic of China "Qualitative detection of Norovirus and Hepatitis A virus in food for export-RT-PCR". Bottled water was selected for food sample testing to determine whether the established CRISPR-SERS biosensor could detect actual food samples. The bottled water used in this study was purchased from a local market. After sample preprocessing according to the SN/T 4784-2017 for virus collection, the samples were prepared for artificial contamination with different concentrations of HAV-cDNA.

As indicated in Table 1, the recovery rate of 82.23–107.99% in bottled water was good and shows that the created biosensor is appropriate for detecting a nucleic acid from this food-derived virus. We also compared the Cas12a-SERS biosensor with the "gold standard" RT-PCR for nucleic acid detection to assess the accuracy of the SERS-based method. As shown in Fig. S1† and Table 1, our SERS method showed good agreement with PCR for the identification of HAV-cDNA in bottled water samples at different levels.

4. Conclusion and discussion

In this work, a highly specific SERS method for identifying nucleic acids from food-borne viruses was developed. This method minimizes the time-consuming DNA amplification phase and improves the sensitivity and selectivity of target DNA detection through a rapid and simple detection process (30 min) by integrating the advantages of SERS detection with CRISPR technology. This CRISPR-SERS biosensor has a selectivity that is noticeably higher than that of conventional SERS tests. Furthermore, it performs well in terms of sensitivity.

The system is available as a programmable platform to detect other viruses by changing the combination of primers and crRNAs. Although HAV-cDNA is used in this paper, current studies have also shown that RNA targeting triggers CRISPR-Cas12a,[58,59] which is expected to directly detect RNA viruses with CRISPR-Cas12a. And because of the different inelastic scattering produced by different molecules, this can be used by designing different signal molecules to simultaneously detect multiple targets in multiple tubes when the sample volume is limited. Considering all of these factors, the CRISPR-SERS biosensor is a promising real-time detection device that offers quick and accurate monitoring of potential risks in the food supply chain.

In this work, CRISPR-SERS is used for indirect target detection. In addition to the target concentration that stimulates the cleavage activity of CRISPR, the concentration of labels is also very important. The plasmon characteristics of noble metal nanoparticles, the reporter molecule's Raman scattering cross-section, and the number of reporter molecules on the nanoparticle surface are the primary factors influencing the SERS signal intensity. Excellent substrate materials have strong SERS responses, so the continuous improvement of substrate manufacturing is still a direction that needs continuous optimization for the practical application of SERS.

Practical applications are severely limited by the fact that the present CRISPR-SERS technology can only detect known DNA sequences, although having significant gains in sensi-

 This journal is © The Royal Society of Chemistry 2024

tivity and specificity. Currently, the primary application of CRISPR/Cas-based SERS technology is *in vitro* nucleic acid detection; however, it remains uncertain if high levels of sensitivity and specificity can be sustained in a complex biological setting. The process of incorporating CRISPR/Cas-based SERS technology into *in vivo* cells for analysis will have a significant impact on the diagnosis, treatment, and prevention of disease.

Author contributions

Conceptualization, Y. L. and Y. Z.; methodology, Y. L. and Y. Z.; validation, Y. Z. and S. Y.; visualization, L. Q. and Z. X.; data curation, Y. L. and H. Y.; software, Y. L. and S. G.; supervision, Y. Z. and S. Y.; writing – original draft, Y. L.; writing – review & editing, Y. L. and Y. Z.; funding acquisition, Y. Z.

Data availability

The data underlying this article will be shared on reasonable request to the corresponding author.

Conflicts of interest

The authors declare no conflict of interest.

Acknowledgements

This research was funded by Shanghai Science and Technology Innovation action plan in the agricultural field of 2022 (22N31900200), The Pioneer Talents Program of Huishan District in 2022 (HRCB20224), Taihu Lake Talents Program of Wuxi City in 2023 (XRCB20234), and Wuxi Science and Technology Innovation Venture Capital in 2022 (Y2022004).

References

1 N. Nasheri, J. Harlow, A. Chen, N. Corneau and S. Bidawid, *J. Food Prot.*, 2020, **83**, 388–396.
2 M. Hajikhani, Y. Zhang, X. Gao and M. Lin, *Trends Food Sci. Technol.*, 2023, **138**, 615–627.
3 H. Ge, Y. Wang and X. Zhao, *Microb. Pathog.*, 2022, **162**, 105306.
4 H. Lee and Y. Yoon, *Food Sci. Anim. Resour.*, 2021, **41**, 1–7.
5 Y. Li, Z. Zhao, Y. Liu, N. Wang, S. Man, L. Ma and S. Wang, *J. Agric. Food Chem.*, 2023, **71**, 13577–13594.
6 P. Vasickova, I. Pavlik, M. Verani and A. Carducci, *Food Environ. Virol.*, 2010, **2**, 24–34.
7 W. Su, D. Liang and M. Tan, *Trends Food Sci. Technol.*, 2021, **113**, 97–109.
8 L. Yin, Y. Li, W. Zhang, X. Han, Q. Wu, Y. Xie, J. Fan and L. Ma, *J. Agric. Food Chem.*, 2023, **71**, 3551–3563.
9 T.-Y. Kim, X. Zhu, S.-M. Kim, J.-A. Lim, M.-A. Woo, M.-C. Lim and K. Luo, *Food Res. Int.*, 2023, **174**, 113502.
10 M. Aladhadh, *Microorganisms*, 2023, **11**, 1111.
11 A. Panwar, V. Bhatnagar, M. Khari, A. W. Salehi and G. Gupta, *Comput. Intell. Neurosci.*, 2022, **2022**, 3045107.
12 L. Wei, P. Indrajit, R. A. Firas, A. S. Ulugbek, M. Ali and S. A. Abed, *Crit. Rev. Anal. Chem.*, 2022, **15**, 1–12.
13 S. Neethirajan, S. R. Ahmed, R. Chand, J. Buozis and É. Nagy, *Nanotheranostics*, 2017, **1**, 272–295.
14 X. Zhu, T.-Y. Kim, S.-M. Kim, K. Luo and M.-C. Lim, *J. Agric. Food Chem.*, 2023, **71**, 15942–15953.
15 P. Van Damme, R. M. Pintó, Z. Feng, F. Cui, A. Gentile and D. Shouval, *Nat. Rev. Dis. Primers*, 2023, **9**, 51.
16 C. V. Raman and K. S. Krishnan, *Nature*, 1928, **121**, 501–502.
17 J. Langer, D. Jimenez de Aberasturi, J. Aizpurua, R. A. Alvarez-Puebla, B. Auguié, J. J. Baumberg, G. C. Bazan, S. E. J. Bell, A. Boisen, A. G. Brolo, J. Choo, D. Cialla-May, V. Deckert, L. Fabris, K. Faulds, F. J. García de Abajo, R. Goodacre, D. Graham, A. J. Haes, C. L. Haynes, C. Huck, T. Itoh, M. Käll, J. Kneipp, N. A. Kotov, H. Kuang, E. C. Le Ru, H. K. Lee, J.-F. Li, X. Y. Ling, S. A. Maier, T. Mayerhöfer, M. Moskovits, K. Murakoshi, J.-M. Nam, S. Nie, Y. Ozaki, I. Pastoriza-Santos, J. Perez-Juste, J. Popp, A. Pucci, S. Reich, B. Ren, G. C. Schatz, T. Shegai, S. Schlücker, L.-L. Tay, K. G. Thomas, Z.-Q. Tian, R. P. Van Duyne, T. Vo-Dinh, Y. Wang, K. A. Willets, C. Xu, H. Xu, Y. Xu, Y. S. Yamamoto, B. Zhao and L. M. Liz-Marzán, *ACS Nano*, 2020, **14**, 28–117.
18 X. X. Han, R. S. Rodriguez, C. L. Haynes, Y. Ozaki and B. Zhao, *Nat. Rev. Methods Primers*, 2022, **1**, 87.
19 I. Pavel, E. McCarney, A. Elkhaled, A. Morrill, K. Plaxco and M. Moskovits, *J. Phys. Chem. C*, 2008, **112**, 4880–4883.
20 E. Papadopoulou and S. E. Bell, *Angew. Chem., Int. Ed.*, 2011, **50**, 9058–9061.
21 S. E. J. Bell and N. M. S. Sirimuthu, *J. Am. Chem. Soc.*, 2006, **128**, 15580–15581.
22 M. Knauer, N. P. Ivleva, X. Liu, R. Niessner and C. Haisch, *Anal. Chem.*, 2010, **82**, 2766–2772.
23 R. Gillibert, J. Q. Huang, Y. Zhang, W. L. Fu and M. Lamy de la Chapelle, *TrAC, Trends Anal. Chem.*, 2018, **105**, 166–172.
24 A. Zhu, S. Ali, T. Jiao, Z. Wang, Q. Ouyang and Q. Chen, *Compr. Rev. Food Sci. Food Saf.*, 2023, **22**, 1466–1494.
25 J. Yoon, N. Choi, J. Ko, K. Kim, S. Lee and J. Choo, *Biosens. Bioelectron.*, 2013, **47**, 62–67.
26 N. Guillot and M. L. de la Chapelle, *J. Quant. Spectrosc. Radiat. Transfer*, 2012, **113**, 2321–2333.
27 L. Tan, C. Y. Effah, S. He, E. K. Drokow, C. Agboyibor, A. Sangmor, H. Yuan, L. Ding, X. Li, T. Sun and Y. Wu, *Vib. Spectrosc.*, 2023, **127**, 103560.
28 L. E. Jamieson, S. M. Asiala, K. Gracie, K. Faulds and D. Graham, *Annu. Rev. Anal. Chem.*, 2017, **10**, 415–437.
29 Y. Xiong, D. Zhang, Y. Hao, Y. Liu and M. Si, *J. Raman Spectrosc.*, 2020, **51**, 46–54.

30 A. Pickar-Oliver and C. A. Gersbach, *Nat. Rev. Mol. Cell Biol.*, 2019, **20**, 490–507.
31 M. Yan and J. Li, *Protein Cell*, 2019, **10**, 783–786.
32 E. J. Sontheimer and L. A. Marraffini, *Science*, 2016, **351**(6276), 920–921.
33 D. S. Chertow, *Science*, 2018, **360**, 381–382.
34 I. El Ouar and A. Djekoun, *Biomed. Pharmacother.*, 2021, **138**, 111487.
35 C. A. Freije and P. C. Sabeti, *Cell Host Microbe*, 2021, **29**, 689–703.
36 X. Zhou, P. A. Renauer, L. Zhou, S.-Y. Fang and S. Chen, *Immunol. Rev.*, 2023, **320**, 199–216.
37 K. Brandt and R. Barrangou, *Annu. Rev. Food Sci. Technol.*, 2019, **10**, 133–150.
38 B. Yin, Q. Zhang, X. Xia, C. Li, W. K. H. Ho, J. Yan, Y. Huang, H. Wu, P. Wang, C. Yi, J. Hao, J. Wang, H. Chen, S. H. D. Wong and M. Yang, *Theranostics*, 2022, **12**, 5914–5930.
39 S. Shang, X. S. Cai and L. S. Qi, *Nat. Comput. Sci.*, 2022, **2**, 533–535.
40 K. O'Leary, *Nat. Med.*, 2022, **123**, 1546–170X.
41 J. S. Chen, E. Ma, L. B. Harrington, M. Da Costa, X. Tian, J. M. Palefsky and J. A. Doudna, *Science*, 2018, **360**, 436–439.
42 J. Zhuang, Z. Zhao, K. Lian, L. Yin, J. Wang, S. Man, G. Liu and L. Ma, *Biosens. Bioelectron.*, 2022, **207**, 114167.
43 S. Y. Li, Q. X. Cheng, J. K. Liu, X. Q. Nie, G. P. Zhao and J. Wang, *Cell Research*, 2018, **28**(4), 491–493.
44 Q. X. Cheng, J. M. Wang, X. Y. Li, Z. L. Zhang, S. Gao, R. B. Cao, G. P. Zhao and J. Wang, *Cell Discovery*, 2018, **4**(1), 20.
45 F. Jia, B. Li, Y. He, Y. Shen, J. Chen, X. Li and Y. Li, *LWT*, 2023, **189**, 115476.
46 J.-H. Choi, M. Shin, L. Yang, B. Conley, J. Yoon, S.-N. Lee, K.-B. Lee and J.-W. Choi, *ACS Nano*, 2021, **15**(8), 13475–13485.
47 Y. Pang, Q. Li, C. Wang, S. Zhen, Z. Sun and R. Xiao, *Chem. Eng. J.*, 2022, **429**, 132109.
48 F. Xu, H. Lai and H. Xu, *Anal. Methods*, 2018, **10**, 3170–3177.
49 X. Wang, X. Guo, J. Chen, C. Ge, H. Zhang, Y. Liu, L. Zhao, Y. Zhang, Z. Wang and L. Sun, *J. Mater. Sci. Technol.*, 2016, **33**, 246–250.
50 T. Duy Vu, D. Thang Nguyen, H. Yen Thi Nguyen, H. Hoang Do, T. Duc Pham, S. Thanh Le and L. Ngoc Vu, *Spectrochim. Acta, Part A*, 2024, **313**, 124137.
51 Y. Liu, Y. Liu, Y. Xing, X. Guo, Y. Ying, Y. Wu, Y. Wen and H. Yang, *Sens. Actuators, B*, 2018, **273**, 884–890.
52 Y. Xu, C. Yang, M. Wang, X. Pan, C. Zhang, M. Liu, S. Xu, S. Jiang and B. Man, *Opt. Express*, 2017, **25**, 16437–16451.
53 H. Yilmaz, D. Yilmaz, I. C. Taskin and M. Culha, *Adv. Drug Delivery Rev.*, 2022, **184**, 114184.
54 D. C. Swarts, J. van der Oost and M. Jinek, *Mol. Cell*, 2017, **66**, 221–233.e4.
55 H. Wu, J.-s. He, F. Zhang, J. Ping and J. Wu, *Anal. Chim. Acta*, 2020, **1096**, 130–137.
56 J. Chakraborty, A. A. Chaudhary, S.-U.-D. Khan, H. A. Rudayni, S. M. Rahaman and H. Sarkar, *ACS Omega*, 2022, **7**, 39562–39573.
57 L. Huang, N. Yuan, W. Guo, Y. Zhang and W. Zhang, *Talanta*, 2023, **252**, 123821.
58 S. R. Rananaware, E. K. Vesco, G. M. Shoemaker, S. S. Anekar, L. S. W. Sandoval, K. S. Meister, N. C. Macaluso, L. T. Nguyen and P. K. Jain, *Nat. Commun.*, 2023, **14**, 5409.
59 J. Zhang, Z. Li, C. Guo, X. Guan, L. Avery, D. Banach and C. Liu, *Angew. Chem., Int. Ed.*, 2024, **63**, e202403123.

This journal is © The Royal Society of Chemistry 2024